Environ Earth Sci (2013) 68:1835–1848
DOI 10.1007/s12665-012-1871-0

ORIGINAL ARTICLE

The effect of heterogeneity of diffusion parameters on chloride transport in low-permeability argillites

Marijke Huysmans · Alain Dassargues

Received: 18 January 2012 / Accepted: 24 July 2012 / Published online: 4 August 2012

Abstract Understanding flow and transport in low-permeability media is very important in the context of nuclear waste disposal, oil and gas reservoirs and long term evolution of groundwater systems. In low-permeability media, transport by diffusion is often the most important mass transport process. This study investigates the effect of the heterogeneity of diffusion parameters on mass transport in low-permeability media. A geostatistical approach for integrating heterogeneity of diffusion parameters in groundwater flow and transport models is proposed and applied to the Toarcian argillites in France which are studied in the framework of feasibility of storing radioactive waste in deep clayey massifs. Stochastic fields of the diffusion parameters of the Toarcian argillites (France) are generated based on 64 measured values of diffusion coefficient and diffusion accessible porosity and used as input for a 3D local-scale groundwater flow and transport model. The chloride concentrations computed by these heterogeneous models are compared to the measured chloride concentrations and to concentrations calculated with a model in which the Toarcian argillites are subdivided into several homogeneous zones. The heterogeneous simulations result in a slightly better correspondence between measured and calculated values and have the additional advantage that the measured diffusion coefficient values in the Toarcian are perfectly honored in the model. This study shows that small-scale variability of diffusion parameters has a significant effect on solute concentrations and omitting this heterogeneity may be a problem in transport calculations in low-permeability media, depending on the specific setting and objectives of the study.

Keywords Diffusion · Geostatistics · Nuclear waste disposal · Chloride transport · Heterogeneity · Porosity

M. Huysmans (✉) · A. Dassargues
Applied Geology and Mineralogy, Department of Earth and Environmental Sciences, Katholieke Universiteit Leuven, Celestijnenlaan 200 E, 3001 Heverlee, Belgium
e-mail: marijke.huysmans@ees.kuleuven.be

A. Dassargues
Hydrogeology and Environmental Geology, Department of Architecture, Geology, Environment, and Civil Engineering (ArGEnCo), Université de Liège, B.52/3 Sart-Tilman, 4000 Liège, Belgium

Introduction

Fluid flow in natural permeable media has been extensively studied and analyzed in several contexts, especially in the development of groundwater resources and the recovery of petroleum. By comparison, less effort has been spent to groundwater flow and transport of pollutants in low-permeability or tight media (Neuzil 1986), which are defined as media with a hydraulic conductivity (K) lower than 10^{-8} m/s. Recently low-permeability layers receive more attention because their low hydraulic conductivities are required for several important geological and environmental applications (Cherry et al. 2006; Bradbury et al. 2006). It has, for example, become clear that aquifer behavior prior to groundwater extraction and aquifer response to groundwater extraction is often influenced by adjoining low-permeability formations (Neuman and Witherspoon 1972; Bredehoeft et al. 1983). It has also been recognized that flow in low-permeability formations plays an important role in the evolution of groundwater flow systems over geologic time. Knowledge of the flow in low-permeability media is also necessary for understanding the geochemical evolution of their pore fluids and solids

(Neuzil 1986). A highly significant motivation for the study of low-permeability environments is geological disposal of toxic waste to minimize their exposure to moving groundwater (Bredehoeft et al. 1978). Sites with low-permeability media are often selected for landfilling of domestic and industrial waste. Nuclear waste disposal is a recent challenge for which low-permeability media are crucial. Extensive research is currently performed on disposal of radioactive waste in deep low-permeability layers. In many countries, a multiple-barrier disposal concept composed of both engineered and natural barriers is proposed to immobilize the radioactive elements and to isolate them from the biosphere (e.g., Barnwart et al. 1997; Mallants et al. 2001; Hummel and Schneider 2005; Schwartz 2009; Acero et al. 2010). The geological layer in which the installation is built is the main barrier that ensures the safety of the disposal installation on the very long term (Ringwood 1985). A better characterization, understanding and modeling of the thermal, chemical, mechanical and hydrogeological behavior of low-permeability layers is an essential part of the solution of the waste problem.

In low-permeability media without significant secondary permeability features such as joints, faults of solution features, transport by diffusion, i.e., transport due to a concentration gradient of solute, is often the most important mass transport process (Mazurek et al. 2011). In permeable aquifers, diffusion is a much slower process than transport by advection and dispersion. In media with a low hydraulic conductivity, however, advection velocities may be very small, so that diffusion may be the dominant transport mechanism under typically encountered conditions of the hydraulic gradient (Goodall and Quigley 1977; Desaulniers et al. 1981, 1986; Crooks and Quigley 1984; Johnson et al. 1989; Shackelford and Daniel 1991; Barone et al. 1992; Remenda et al. 1996; Ball et al. 1997; Patriarche et al. 2004b; Huysmans and Dassargues 2005; Mazurek et al. 2011).

The main diffusion parameters are the effective diffusion coefficient and the diffusion accessible porosity as the diffusive mass flux in porous media is given by:

$$F = -\eta D_e \nabla C \quad (1)$$

where F is the diffusive mass flux (kg/m^{2}s), η is the diffusion accessible porosity (−), D_e is the effective diffusion coefficient (m^2/s) and C is the solute concentration (kg/m^3).

The diffusion accessible porosity is not always equal to the total porosity but may be smaller. Only a fraction of the total water-filled porosity is available for diffusive transport. This is caused by size-exclusion effects, i.e., some pores are narrower than the ion size, and by the permanent structural negative charge on the clay surface, which can cause negatively charged ions to be excluded from the narrower interparticle spaces of the clay (Horseman et al. 1996).

As diffusion is such an important process in low-permeability media, spatial variability of the diffusion parameters may have a significant effect on mass transport in such media. Huysmans and Dassargues (2006, 2007) investigated the effect of spatial variability of diffusion parameters on modeled radionuclide concentrations in the Boom Clay (Belgium). This analysis showed that the heterogeneity of the diffusion parameters has a much larger effect on the calculated output radionuclide fluxes than the heterogeneity of hydraulic conductivity in the low-permeability medium under study. The results of this former study could not however be verified with measured concentrations or fluxes since in that study, predicted radionuclide transport was modeled that could result from hypothetical disposal of high-level nuclear waste.

In the present study, the effect of the heterogeneity of diffusion parameters on mass transport in low-permeability media is presented as a case study where measured chloride concentrations are available. The effect of spatial variability of diffusion coefficient and diffusion accessible porosity on chloride transport in the Toarcian argillites (France) during the last 53 million years is modeled. Comparison of measured concentrations with modeled concentrations from heterogeneous and homogeneous transport models quantifies the effect of small-scale variability of diffusion parameters on solute concentrations.

Methodology

The method is based on a stochastic approach. Stochastic fields of the diffusion parameters of the Toarcian argillites (France) are generated based on geostatistical simulation using measured values and used as input for a 3D local-scale groundwater flow and transport model. The method consists in the following successive steps: (1) data collection on diffusion parameters, (2) division of the model domain into statistically stationary zones, (3) variography, (4) cross-validation, (5) stochastic simulation of the diffusion parameters and (6) hydrogeological modeling.

Study site

The Domerian and Toarcian argillites were deposited in a Mesozoic marine basin on the Southern border of the French Massif Central. The unit of interest is a 250 m thick, sub-horizontal layer of argillites and marls of Toarcian and Domerian age, located between two aquifer limestone and dolomite layers of Carixian and Aalenian age (Fig. 1). An old railway tunnel of 2 km long at the Tournemire site (Aveyron, France) gives convenient access to the Toarcian layers (Bonin 1998). The Domerian Series consists of 40 m of marl and argillite (Boisson et al. 2001).

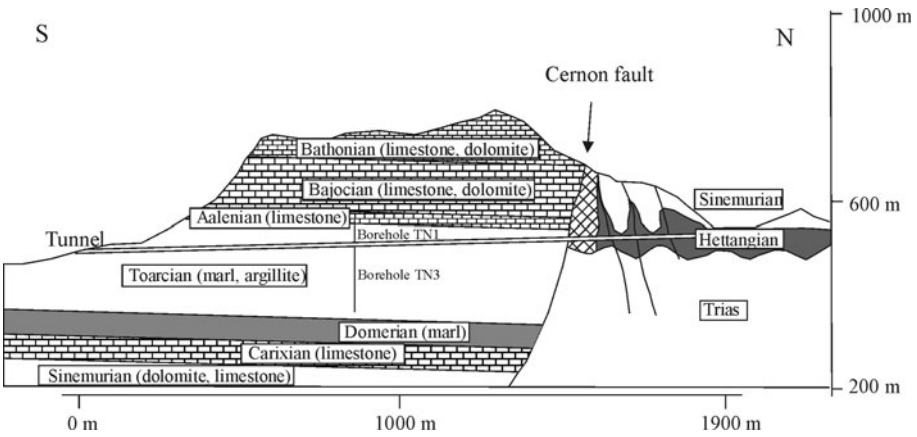

Fig. 1 Vertical cross section of the Tournemire massif showing the Trias and Jurassic successions after Patriarche et al. (2004a)

The Toarcian Series can be subdivided into the Lower, Middle and Upper Toarcian. At the Tournemire Tunnel site, the Lower Toarcian consists of 20 m of paper shale, the Middle Toarcian consists of 25 m of marls and the Upper Toarcian consists of 160 m of grey–blue argillites (Patriarche et al. 2004a).

The Toarcian argillites are characterized by a very small porosity of 6–9 % (Bonin 1998) and a low natural water content of 3–5 % (Boisson et al. 2001). Measured hydraulic conductivity values exhibit a large range: $K = 10^{-15}$ to 10^{-14} m/s for laboratory measurements on small samples and $K = 10^{-13}$ to 10^{-14} m/s for in situ measurements (Bonin 1998). Permeability measurements on centimeter-sized samples yield results about one order of magnitude lower than in situ measurements which indicates that hydraulically active fractures may exist in large volumes and go unnoticed in smaller volumes. On the Tournemire site, natural discontinuities are present at different scales. These discontinuities are related to two important tectonic episodes: extension in the Jurassic and compression in the Paleogene. The largest discontinuity observed on the Tournemire site is the Cernon fault, which is hydraulically active and played an important role in the circulation of fluids (Bonin 1998). Several secondary faults associated with fractured zones of several meters are also observed in the tunnel. On a smaller scale, three types of discontinuities are observed: principal planes, secondary planes and microfissures. The principal planes are decimeter-scale planes with an aperture of a few centimeters filled with calcite. The secondary planes are meter-scale planes with an aperture of a few millimeters filled with calcite. The microfissures are decimeter- to meter-scale planes with very fine apertures of 1 mm or less and are also filled with calcite. The principal planes have a well-defined orientation, while the secondary planes and microfissures have a much larger range of orientations (Boisson et al. 1998).

Given these geological considerations, the IRSN (French Institution for Radioprotection and Nuclear Safety, formerly IPSN) selected the Tournemire tunnel site for installing an underground experimental facility. The IRSN is in charge of an independent expertise for industrial projects, e.g., for Andra (Agence Nationale pour la gestion des déchets radioactifs) projects. In order to conduct methodological research on the feasibility of storing radioactive waste in deep clayey massifs, the IPSN selected in 1988 the argillaceous units (Upper Lias) of the Tournemire massif (Aveyron, southern France) for installing an underground experimental facility.

Data collection

Sixty-four diffusion coefficient and diffusion accessible porosity measurements for chloride (Fig. 2) are available from cores from the TN1 and TN3 boreholes at the Tournemire site (Patriarche et al. 2004a). These values were measured by executing and modeling diffusion experiments on rock samples. No information about the potential error on these measurements is available as Patriarche et al. (2004a) state that "because of the low number of water samples collecting during each experiment and due to the fact that porosity was derived only using the water content, they were unable to calculate the uncertainties on pore water chloride concentrations or chloride diffusion coefficients". More information on the measurement protocol can be found in Patriarche et al. (2004a). The diffusion accessible porosity was not measured directly but determined as the total porosity multiplied by a factor 0.3 corresponding to the estimated proportion of accessible pores for chloride (Patriarche et al. 2004a). Although some uncertainty is associated with this 0.3 factor and although this factor may be non-constant, this choice was made to be consistent with the work of Patriarche et al. (2004a) to allow comparison of both studies. The correlation coefficient of D_e and η is −0.074. The two diffusion variables are thus uncorrelated as confirmed by the scatterplot (Fig. 3).

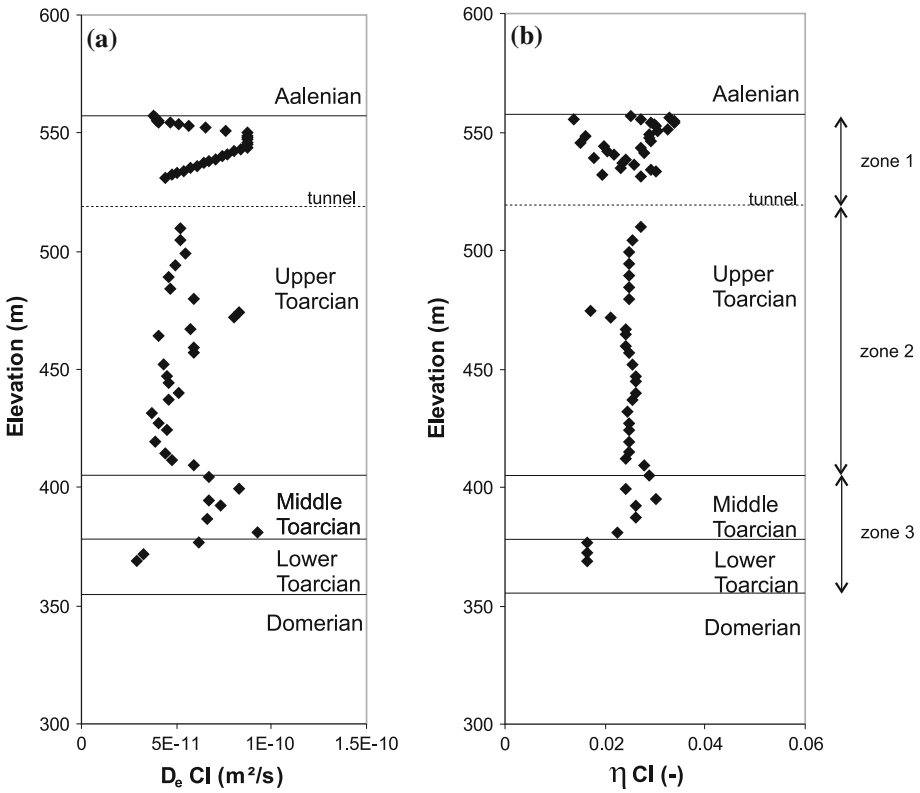

Fig. 2 **a** Measured chloride diffusion coefficient and **b** measured chloride diffusion accessible porosity of the Toarcian argillites in the TN1 and TN3 boreholes

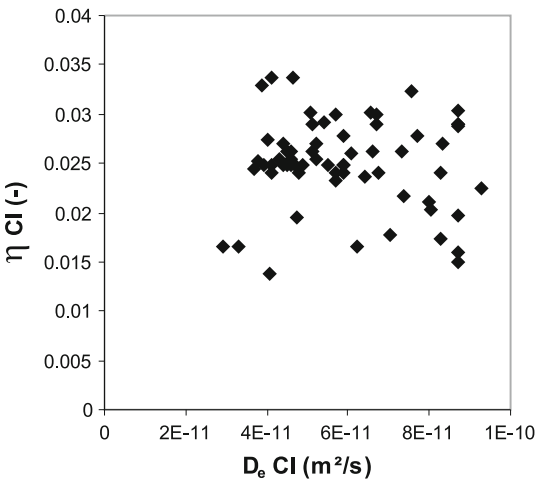

Fig. 3 Scatterplot of De and η of the Toarcian argillites in the TN1 and TN3 boreholes

Division of the model domain into stationary zones

Geostatistical simulation makes strong assumptions of stationarity in the mean and variance over the domain of interest. Geological nature usually does not reflect these assumptions and the model area is therefore often subdivided into stationary regions that have some common geological controls and similar statistical properties (Larrondo and Deutsch 2004). Plots of the spatial distribution of the data and univariate statistical analysis (histograms, mean values and variances) provide the tools to detect the presence of different stationary zones. Neglecting the presence of different stationary zones can result in unclear variogram structures and over- or underestimation of the mean and/or variance of hydraulic conductivity in certain zones. The advantage of subdividing the domain into stationary zones should be weighed against the disadvantage of reducing the number of data points per zone.

The plots of the spatial distribution of the diffusion coefficient and the diffusion accessible porosity (Fig. 2) are studied to detect the potential presence of different statistically stationary zones. The diffusion coefficient shows similar values and variability over the total thickness of the Toarcian argillites (Table 1). The diffusion accessible porosity has a much lower variability in the lower part of the Upper Toarcian comparing to the upper part of the Upper Toarcian and the Middle and Lower Toarcian. The Toarcian is therefore subdivided into three zones:

Table 1 Statistics of D_e and η in the three zones

	Zone 1 (520–557 m)	Zone 2 (405–520 m)	Zone 3 (355–405 m)
Average D_e	6.44E−11	4.82E−11	6.32E−11
Variance D_e	3.21E−22	4.31E−23	3.90E−22
Average η	0.0258	0.0250	0.0235
Variance η	3.15E−05	6.88E−07	2.81E−05

(1) the upper part of the Upper Toarcian (520–557 m), (2) the lower part of the Upper Toarcian (405–520 m) and (3) the Middle and Lower Toarcian (355–405 m). Table 1 shows the statistics in each of these three zones. Taking these three zones of different variability together would lead to variograms with an unclear spatial structure and simulations with too large variability in the middle part of the Toarcian argillites. The advantages of dividing the domain into three zones are further examined using cross-validation techniques in Sect. 2.5.

Variography

Geostatistics provides a set of tools to describe the spatial continuity that is an essential feature of many natural phenomena. Definitions of geostatistical estimators are covered extensively by Isaaks and Srivastava (1989) and Deutsch and Journel (1998). The most familiar geostatistical estimator is the semivariogram. The experimental semivariogram is calculated as half of the average squared difference between variable values separated by a lag vector **h**:

$$\gamma_{ii}(h) = \frac{1}{2N(h)} \sum_{\alpha=1}^{N(h)} (z_i(\mathbf{x}_\alpha + \mathbf{h}) - z_i(\mathbf{x}_\alpha))^2 \quad (2)$$

where $N(\mathbf{h})$ is the number of pairs and $z_i(\mathbf{x})$ is a regionalized variable. The semivariogram can be understood as the sample variance described as a function of spatial separation. Low semivariogram values indicate a high degree of correlation between variable values separated by the lag vector, while high semivariogram values indicate a low degree of correlation. Experimental semivariograms and cross-variograms are usually modeled with an analytical variogram model so that (1) all the variogram values needed by the kriging system are provided and (2) the restriction of positive definiteness of the kriging matrices is satisfied (Isaaks and Srivastava 1989). Common variogram models are the nugget effect model, the spherical model, the exponential model, the Gaussian model and the linear model. More information on variogram models can be found in geostatistics textbooks (e.g., Isaaks and Srivastava 1989).

Experimental variograms of D_e and η are calculated using the GAMV module of GSLIB (Deutsch and Journel 1998) for the complete dataset of the TN1 and TN3 boreholes (Fig. 4a) and for each zone separately (Fig. 4b–d). Since D_e and η are uncorrelated, they are treated as two separate parameters and should not be modeled with similar variogram models. The D_e variogram of the Toarcian argillites is modeled with a spherical model with a range of 8.5 m. The η variogram is modeled with a pure nugget model. This lack of spatial structure is a consequence of combining data from zones with different variability. The D_e variogram of zone 1 is modeled with a Gaussian model with a range of 8.5 m. The η variogram is a pure nugget variogram corresponding to the erratic η values in zone 1 (see Fig. 2b). The two porosity outliers in zone 2 at an elevation of approximately 475 m (Fig. 2b) are removed from the dataset for variogram calculation and modeling since such outliers result in very large variogram values for the first lag and obscure the spatial structure. These values are however added back to the dataset after variogram calculation and are used in the simulations procedure. The D_e variogram of zone 2 is modeled with a spherical model with a range of 8 m. The η variogram of zone 2 is modeled with a spherical model with a range of 14 m. In zone 3, the D_e and η variograms are modeled with Gaussian models with a range of 9.5 and 40 m, respectively. For zone 3, this means that the vertical range of the η variogram is almost equal to the thickness of the zone. This indicates a large spatial continuity of η in that zone. The sill values of the D_e and η variograms are significantly smaller in zone 2 than in zones 1 and 3. Some of the variograms have a rather erratic behavior. This is attributed to the relatively low amount of data per zone and the presence of periodicities in the data that cannot be captured by standard variogram models. The variograms are however considered accurate enough for application of the methodology since (1) cross-validation (see "Cross-validation") shows that geostatistical estimation using these variograms performs well and (2) the resulting simulated realizations (see "Stochastic simulation of the diffusion parameters") reproduce the general trends and variability of the original data.

Cross-validation

Cross-validation is a technique to evaluate alternative models used for kriging. Kriging is a weighted linear estimator in which the attribute value is estimated as a linear combination of different data values. The weights of the data points are assigned considering (1) the closeness of the location being estimated, (2) the redundancy between the data values, (3) anisotropy and (4) the magnitude of continuity or variability. The weights are calculated using the modeled variograms and/or cross-variograms. For more information on kriging and co-kriging, the reader is referred to a geostatistics textbook (e.g., Isaaks and Srivastava 1989).

In cross-validation analysis, each measured point in a data set is individually removed from the set and its value is then estimated by kriging. This provides estimated versus actual values for each sample location that can be compared. In this section, cross-validation techniques are used to investigate the advantage of subdividing the domain into three zones. The diffusion parameters are

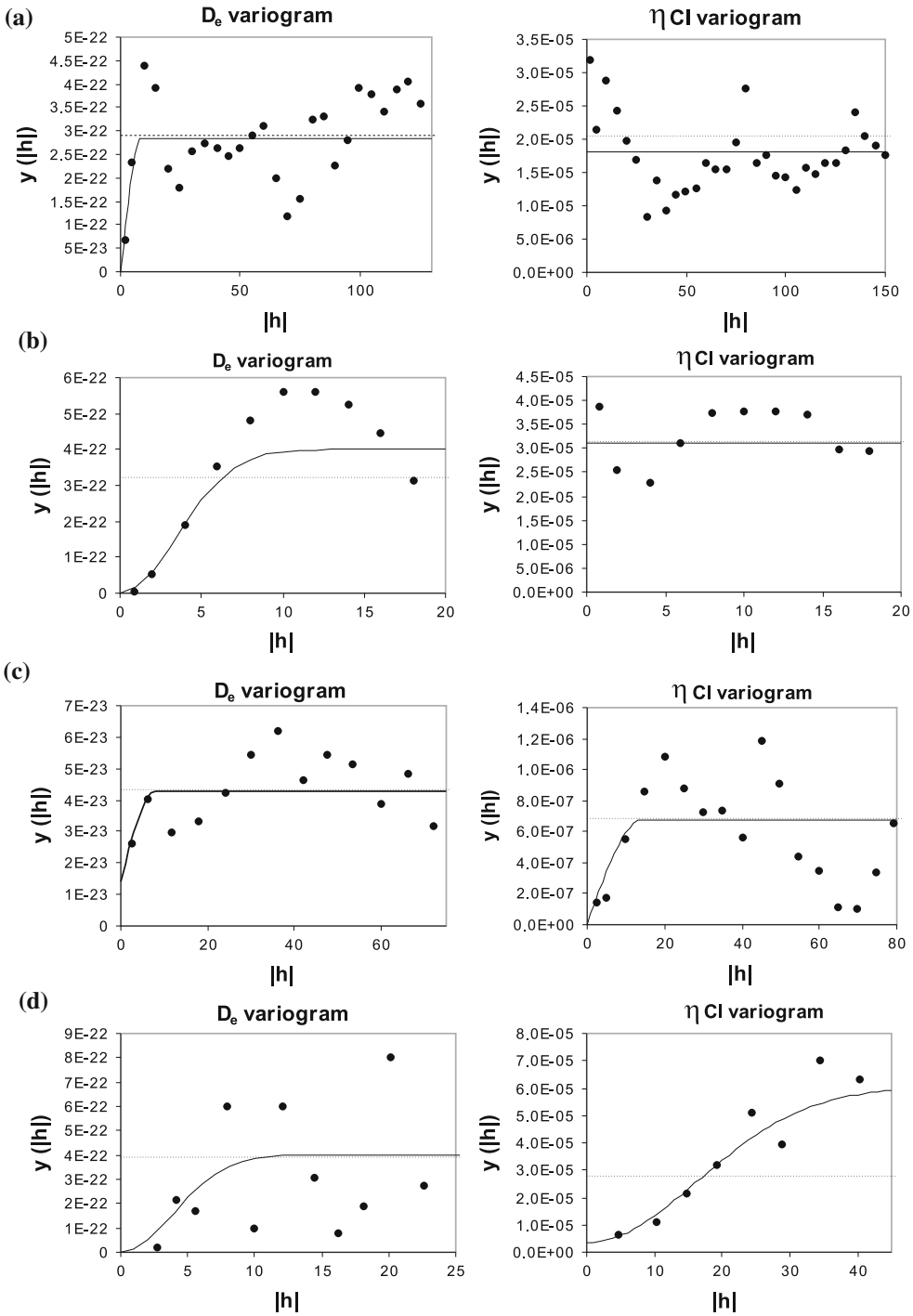

Fig. 4 **a** Experimental and modeled variograms of De and η versus lag distance h (m) in the Toarcian argillites in the TN1 and TN3 boreholes, **b** in zone 1, **c** in zone 2 and **d** in zone 3

estimated using (1) the variograms of the complete dataset and (2) the variograms of the three different zones. The estimated versus measured values are compared to evaluate the advantage of subdividing the domain into three zones.

Figures 5 and 6 respectively show the kriging estimates and the kriging residuals of the diffusion coefficient of the Toarcian argillites obtained by cross-validation without and with subdivision into three zones. Figure 7 shows the measured versus estimated values. Table 2 shows the statistics of the D_e residuals. Subdividing the domain results in a slightly lower standard deviation of the residuals, although the correlation coefficient of the measured and estimated values of the Toarcian argillites (0.91) and of each of the zones separately (0.997, 0.84 and 0.72 respectively) are almost unaffected by subdivision of the domain.

Figures 8 and 9, respectively, show the kriging estimates and the kriging residuals of the diffusion accessible porosity

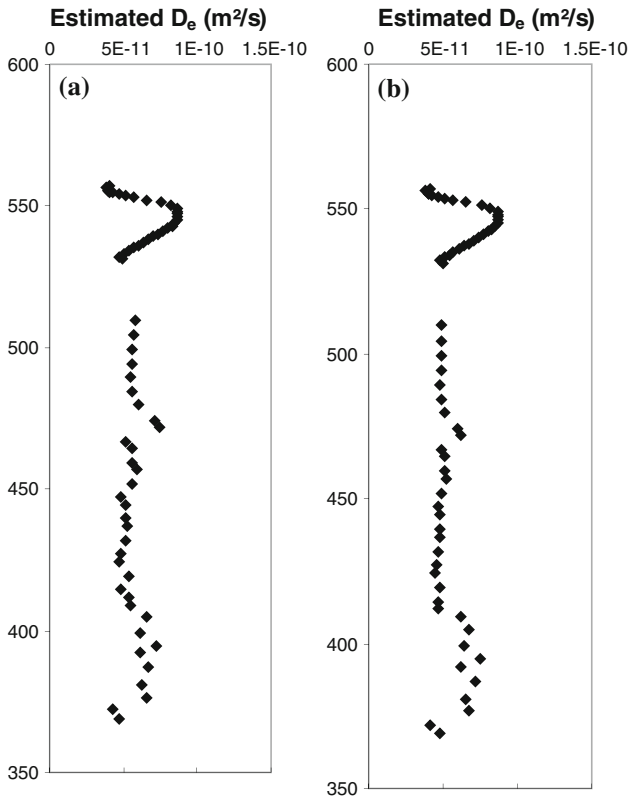

Fig. 5 Cross-validation results: kriging estimates of the diffusion coefficient of the Toarcian argillites versus depth in the TN1 and TN3 boreholes **a** without subdivision of the domain and **b** with subdivision into three zones

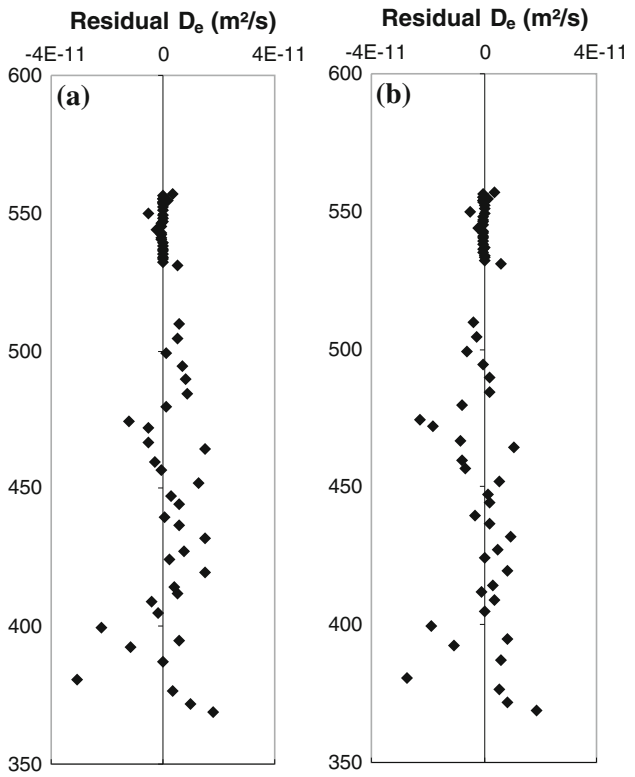

Fig. 6 Cross-validation results: kriging residuals of the diffusion coefficient of the Toarcian argillites versus depth in the TN1 and TN3 boreholes **a** without subdivision of the domain and **b** with subdivision into three zones

of the Toarcian argillites obtained by cross-validation without and with subdivision into three zones. Since η has a pure nugget variogram in the case that the domain is not subdivided, the residuals are equal to the arithmetic mean of the data minus the measured value. The kriging residuals thus show the same variability as the original data. For the second case with subdivision into three zones, only zone 1 is modeled by a pure nugget variogram. The residuals of zone 2 and 3 improve significantly after subdivision of the domain: the residuals have a lower standard deviation and the correlation coefficient between measured and estimated values is much higher (Fig. 10; Table 3). The correlation coefficient increases from 0 to 0.46 for the whole domain, from 0 to 0.81 for zone 2 and from 0 to 0.83 for zone 3. The correlation coefficient of zone 1 is unaffected by subdivision of the domain since the variogram of this zone is modeled by a pure nugget variogram in both cases, i.e., without and with subdivision.

Cross-validation shows that subdivision of the domain improves the estimation of the diffusion accessible porosity and the diffusion coefficient in the Toarcian argillites. Therefore, the stochastic simulations of D_e and η are carried out in the three zones separately with different variograms for each zone.

Stochastic simulation of the diffusion parameters

The simulation algorithm used in this study is based on direct sequential simulation with histogram reproduction (Oz et al. 2003). This direct sequential simulation does not require any Gaussian assumption and simulates directly the data space. A large number of equally probably random realizations of the clay layer are generated, using the modeled variograms. It is assumed that the properties of the Toarcian argillites do not vary significantly in the horizontal direction given the horizontal layering observed and one-dimensional vertical realizations of the diffusion coefficient and the diffusion accessible porosity are generated. Figure 11 shows three random realizations of the diffusion coefficient of chloride and Fig. 12 shows three random realizations of the diffusion accessible porosity of chloride that illustrate the degree of similarity and dissimilarity between different realizations. All generated realizations respect the modeled variograms.

Hydrogeological modeling

Each of the simulated fields of diffusion coefficient and diffusion accessible porosity is used as input to a

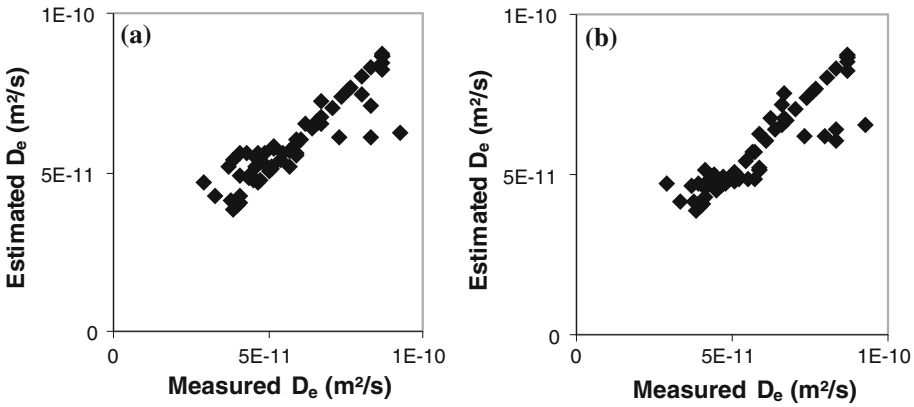

Fig. 7 Scatterplots of measured diffusion coefficient versus estimated diffusion coefficient of Toarcian argillites versus depth in the TN1 and TN3 boreholes **a** without subdivision of the domain and **b** with subdivision into three zones

Table 2 Statistical properties of the D_e kriging residuals of the Toarcian argillites in the TN1 and TN3 boreholes

	No subdivision	Subdivision into three zones
Arithmetic mean of residuals	1.07E−12	−6.35E−13
Standard deviation of residuals	7.49E−12	7.30E−12
Minimum of residuals	−3.09E−11	−2.76E−11
Maximum of residuals	1.78E−11	1.85E−11
Correlation coefficient of measured and estimated De values	0.91	0.91

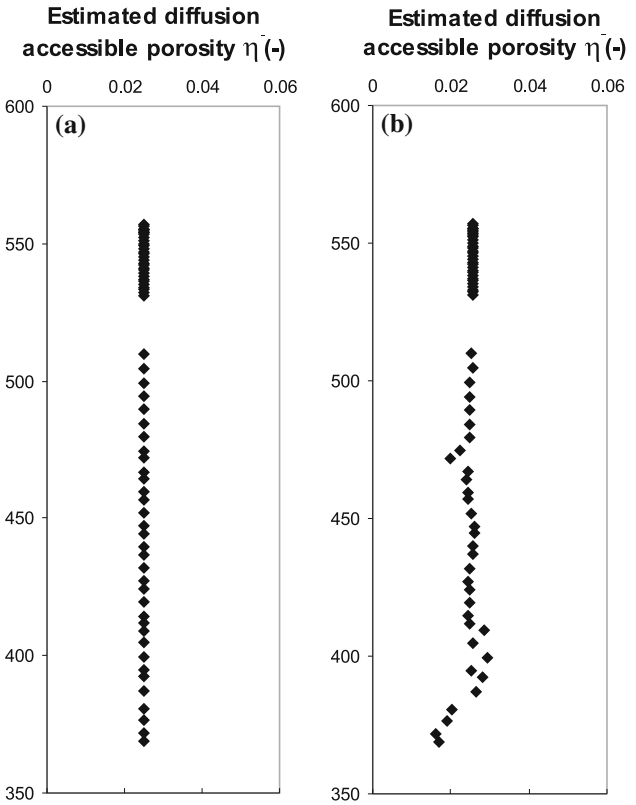

Fig. 8 Cross-validation results: kriging estimates of the diffusion accessible porosity of the Toarcian argillites versus depth in the TN1 and TN3 boreholes **a** without subdivision of the domain and **b** with subdivision into three zones

groundwater flow and mass transport model. In a Monte Carlo approach, the hydrogeological model is run N times for each of the N simulated input fields to obtain N sets of results. All models are run with FRAC3DVS, a simulator for 3D groundwater flow and solute transport in porous, discretely fractured porous or dual-porosity formations (Therrien and Sudicky 1996; Therrien et al. 2003). Statistical analysis of the N sets of results provides predictive frequency distributions of the response variables, e.g., concentration levels or solute mass fluxes. Transport by advection and diffusion is modeled.

A hydrogeological flow and transport model is constructed and calibrated to simulate transport of naturally present chloride over the past 53 million years. It is assumed that the initial pore water in the argillites was seawater trapped during deposition with high chloride content (Patriarche et al. 2004b). Fresh water from precipitation with low chloride content began circulating in the karstic aquifers above and below 53 million years ago and influenced the chloride concentration in the argillites. A comparison is made between the measured profiles of chloride in the low-permeability layers and the calculated profiles obtained by numerical modeling. The aim of this exercise is to investigate whether a model that incorporates parameter heterogeneity in a rigorous geostatistical way performs better at reproducing the measured profiles of chloride compared to the model of Patriarche et al. (2004b) in which the Toarcian argillites are subdivided in three homogeneous horizontal zones.

The hydrogeological model is very similar to the model developed by Patriarche et al. (2004b) in terms of boundary and initial conditions and some parameter values. The model is a one-dimensional vertical model with a height of 278 m. The lower and upper aquifers are partially included in the model. The top of the Carixian unit corresponds to the lower

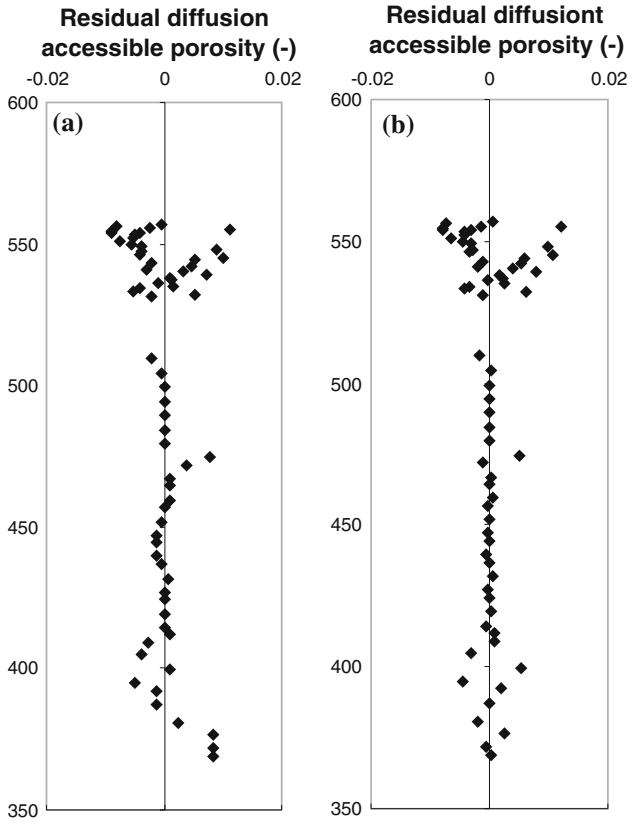

Fig. 9 Cross-validation results: kriging residuals of the diffusion accessible porosity of the Toarcian argillites versus depth in the TN1 and TN3 boreholes **a** without subdivision of the domain and **b** with subdivision into three zones

limit of the low-permeability layers and is represented at the lower boundary as a unit of 1 m thick. The Aalenian aquifer is represented in the model as a 17 m thick unit that corresponds to the present phreatic zone (Fig. 1).

Hydraulic conductivity values are taken from Patriarche et al. (2004b): $K = 10^{-9}$ m/s in the Aalenian, $K = 0.8 \times 10^{-14}$ m/s in the upper and middle part of the Upper Toarcian, $K = 2.3 \times 10^{-14}$ m/s in the lower part of the Upper Toarcian, $K = 2 \times 10^{-14}$ m/s in the Middle Toarcian, $K = 0.8 \times 10^{-14}$ m/s in the Lower Toarcian and $K = 0.9 \times 10^{-14}$ m/s in the Domerian. Patriarche et al. (2004b) propose that the vertical diffusion coefficient is half of the omnidirectional diffusion coefficient. Therefore, the vertical diffusion coefficient in the Toarcian layers is taken as half of the stochastically simulated omnidirectional diffusion coefficient values to be consistent so that the heterogeneous models of this study can be compared with the model results from Patriarche et al. (2004b). The ratio between vertical and omnidirectional diffusion coefficients is however still a large source of uncertainty and may be investigated in further studies. The diffusion coefficient in the Aalenian and Domerian layers is initially taken equal to the calibrated values of Patriarche et al. (2004b), i.e., $D_e = 8 \times 10^{-11}$ m/s in the Aalenian and 2.5×10^{-12} m^2/s in the Domerian. These values are calibrated afterwards in a heterogeneous model with simulated diffusion coefficient in the Toarcian. Diffusion accessible porosity is stochastically simulated in the Toarcian layers and respectively equal to 5 % in the Aalenian and 1.2 % in the Domerian. The specific storage coefficient is 5×10^{-6} m^{-1} (Patriarche et al. 2004b).

Patriarche et al. (2004b) derived boundary and initial conditions for flow and transport from the geological history of the region. It is assumed that the hydraulic heads of both aquifers were initially equal, and that the hydraulic head of the lower aquifer uniformly decreased during the

Table 3 Statistical properties of the η kriging residuals of the Toarcian argillites in the TN1 and TN3 boreholes

	No subdivision	Subdivision into three zones
Arithmetic mean of residuals	−3.75E−06	7.29688E−05
Standard deviation of residuals	0.0045	0.0040
Minimum of residuals	−0.0088	−0.0080
Maximum of residuals	0.011	0.012
Correlation coefficient of measured and estimated η values	3.66E−15	0.46

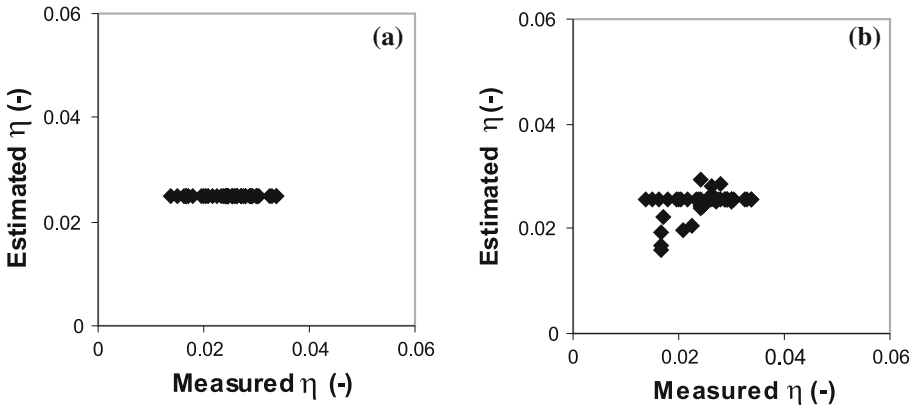

Fig. 10 Scatterplots of measured diffusion accessible porosity η versus estimated diffusion accessible porosity η of Toarcian argillites versus depth in the TN1 and TN3 boreholes **a** without subdivision of the domain and **b** with subdivision into three zones

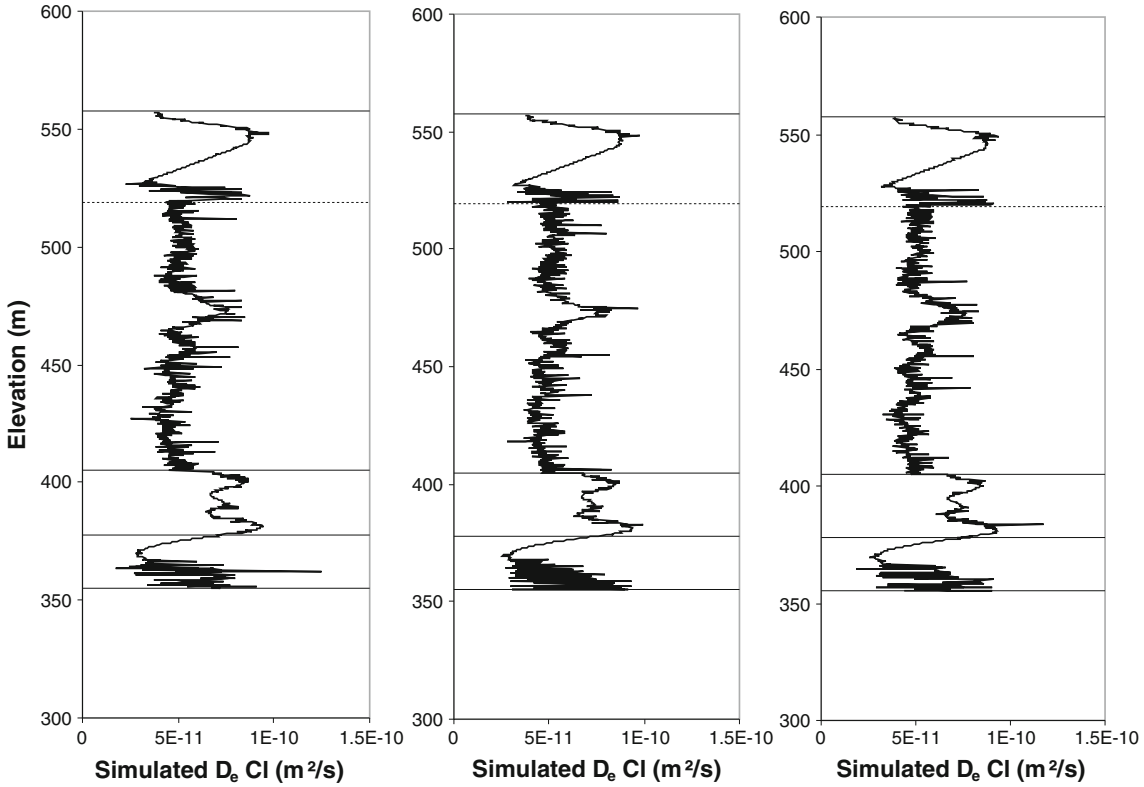

Fig. 11 Three realizations of diffusion coefficient of the Toarcian argillites

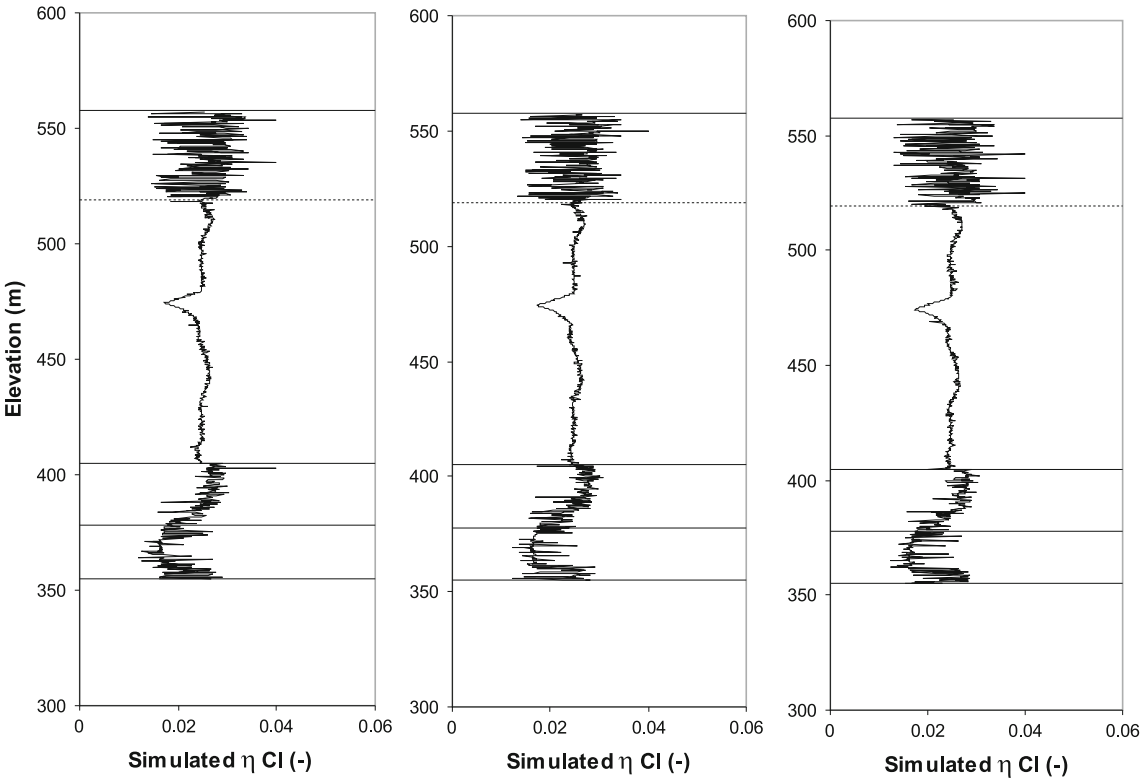

Fig. 12 Three realizations of diffusion accessible porosity of the Toarcian argillites

last 3 million years due to erosion and lowering of the sea level, reaching its present-day value. The initial hydraulic heads of the aquifers are equal to 602 m. The hydraulic head of the lower boundary steadily decreases during the last 3 million years at a rate of 46 m/Ma, reaching a value of 463 m at the present time (Patriarche et al. 2004b). The boundary and initial conditions for transport are based on the assumption that the initial pore water in the argillites is seawater trapped during deposition of the clayey layers. Fresh water from precipitation began circulating in the karstic aquifers above and below 53 million years ago. The initial chloride concentration in the low-permeability layers is assumed equal to the present concentration of chloride in seawater ($C_0 = 20 \times 10^3$ mg/l) and the assumed constant concentration in the aquifers is equal to the present-day chloride concentration in the aquifers ($C = 5$ mg/l).

The diffusion coefficients of the Aalenian and Domerian formation are calibrated following a quadratic calibration criterion

$$S = \frac{1}{n}\sum_{1}^{n}\frac{(C_{\text{measured}} - C_{\text{modelled}})^2}{(C_{\text{measured}})^2} \quad (3)$$

where n is the number of measurements. With this criterion, which is also used in Patriarche et al. (2004b), discrepancies between measured and modeled concentration values are more heavily penalized for small concentration values than for large concentration values since Patriarche et al. (2004b) found that larger measured concentration values are associated with larger errors. After calibration of the diffusion coefficients of the Aalenian and Domerian formation, the model is run for ten different random combinations of simulations of the diffusion coefficient and the diffusion accessible porosity with FRAC3DVS, a simulator for 3D groundwater flow and solute transport in porous, discretely fractured porous or dual-porosity formations (Therrien and Sudicky 1996; Therrien et al. 2003). Although FRAC3DVS enables incorporating discrete fractures, no fractures are present in the current model. Only ten realizations are generated since the results show that the difference between the calculated radionuclide fluxes of the ten different simulations is very small. The results of this model are compared with the results of the zoned model of Patriarche et al. (2004b).

Results

The calibrated diffusion coefficients of the Domerian and Aalenian formations in the heterogeneous model are respectively 1.56×10^{-11} m^2/s (2.5×10^{-12} m^2/s in Patriarche et al. 2004b) and 4.28×10^{-11} m^2/s (8×10^{-11} m/s in Patriarche et al. 2004b). The calibrated diffusion coefficient of the Aalenian formation is of the same order of magnitude as the calibrated value of Patriarche et al. (2004b), while the calibrated diffusion coefficient of the Domerian formation is much larger than the value proposed by Patriarche et al. (2004b). Since no measurements of the chloride diffusion coefficient are available in the Domerian, this value has a large uncertainty.

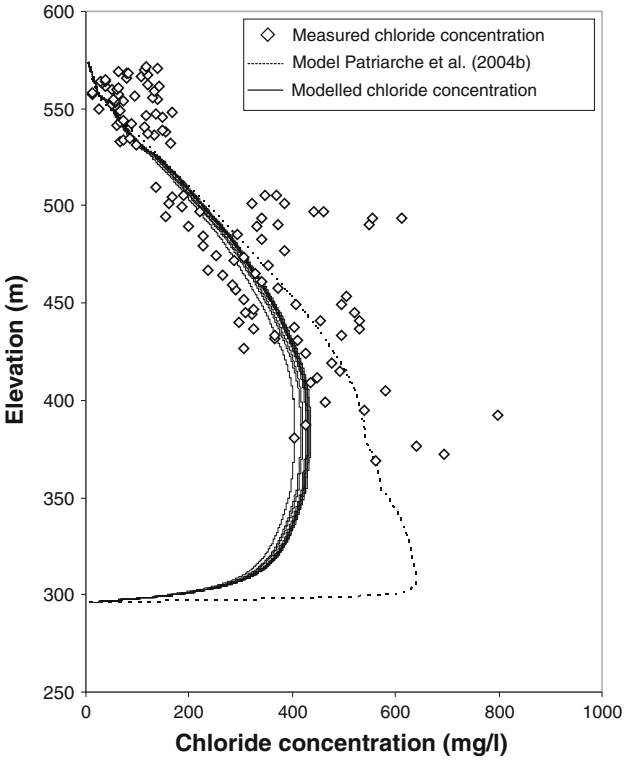

Fig. 13 Vertical profile of experimental and calculated chloride concentrations at the present time

Figure 13 shows a vertical profile of experimental and calculated chloride concentrations at the present time. The figure shows the modeled concentration values of Patriarche et al. (2004b) and the modeled concentration values using ten different heterogeneous simulations of the diffusion coefficient of the Toarcian. The results for the ten heterogeneous simulations are similar to the model of Patriarche et al. (2004b) in the Aalenian and upper part of the Toarcian but are different for the lower part of the Toarcian and the Domerian where the heterogeneous model results in lower chloride concentration values. Differences up to 400 mg/l are noted. The value of the calibration criterion S is 0.2179 of the model of Patriarche et al. (2004b) and the S values of the ten simulations vary between 0.2042 and 0.2067.

A sensitivity analysis is performed to analyze the effect of input parameter changes on the model results. Starting from one of the ten models with a heterogeneous

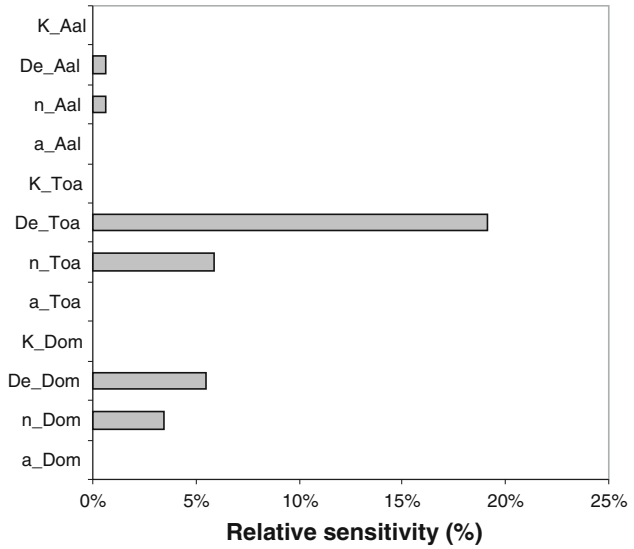

Fig. 14 Relative sensitivity of the *calibration error S* to hydraulic conductivity, diffusion coefficient, diffusion accessible porosity and dispersivity of the Toarcian, Aalenian and Domerian layers

D_e and η, the relative sensitivity of each parameter P is calculated as

$$\frac{S(110\ \%P) + S(90\ \%P)}{2 \times S(100\ \%P)} \tag{4}$$

where $S(110\ \%P)$ is the S criterion of a model where parameter P has a value 10 % larger than the base value, $S(90\ \%P)$ is the S criterion of a model where parameter P has a value 10 % smaller than the base value and $S(100\ \%P)$ is the S criterion of the base model. Figure 14 shows the relative sensitivity of the calibration error S to hydraulic conductivity, diffusion coefficient, diffusion accessible porosity and dispersivity of the Toarcian, Aalenian and Domerian layers. The calibration error S is most sensitive to the diffusion parameters of the Toarcian and the Domerian while the hydraulic conductivity and dispersivity of the different layers have almost no effect of the model results. This result confirms the large importance of transport by diffusion compared to transport by advection.

Discussion

The value of the calibration criterion S is slightly lager in the model of Patriarche et al. (2004b) compared to the ten heterogeneous simulations. It may seem odd that the heterogeneous models result in lower S values since the figure seems to indicate that the higher chloride concentrations are much better reproduced by the model of Patriarche et al. (2004b). This can be explained by the choice of the calibration criterion: discrepancies between measured and modeled concentration values are more heavily penalized for small concentration values than for large concentration values since larger measured concentration values are associated with larger errors. It is thus much more important to reproduce the small chloride concentrations correctly than to reproduce the larger chloride concentrations. The heterogeneous simulations thus result in a slightly better correspondence between measured and calculated values according to the quadratic S criterion.

All models, the heterogeneous simulations and the model of Patriarche et al. (2004b) seem to have problems to accurately reproduce data in the lower part of the sequence. This may be related with the uncertainties about the lower boundary condition of the model. For future work, it may be necessary to derive a more accurate hydrogeological history of the massif, and to obtain more data on chloride concentrations and diffusion coefficients at these lower levels in order to better-constrain the model. Additionally, a two-dimensional model including lithologic heterogeneities, fractures and calcareous nodules would possibly result in a better representation of horizontal variations of chloride concentrations. Additional research on other sources of uncertainty such as the anisotropy ratio of diffusion coefficients and the relation between total porosity and diffusion accessible porosity would also be beneficial to a better comprehension of chloride concentrations at the study site.

Conclusion

The large difference between the calculated concentrations resulting from a model with explicit incorporation of small-scale heterogeneity of the diffusion parameters and the calculated concentrations from a model with homogeneous zones suggests that small-scale variability of the diffusion parameters may have a significant effect on output concentrations. Moreover, the heterogeneous simulations result in a slightly better correspondence between measured and calculated values. Disregarding the heterogeneity of diffusion parameters can result in a problem, depending on the specific setting and objectives of an analysis. Incorporating this heterogeneity can be done using geostatistical simulation as shown in this study. This approach allows simulating maps reproducing the global patterns of spatial continuity and the global statistics showing the nature of local variability. This approach has the additional advantage that the measured diffusion coefficient and porosity values are perfectly honored in the model.

This study thus confirms the findings of Huysmans and Dassargues (2006) who found that disregarding the heterogeneity of the diffusion parameters, i.e., the diffusion coefficient and diffusion accessible porosity can be

problematic in transport models of low-permeability media. This is logical since in low-permeability media, transport by diffusion is an important transport mechanism, often more dominant than advection. If diffusion is the dominant transport mechanism, the solute concentrations and fluxes may be very sensitive to changes in diffusion parameters. While the results of Huysmans and Dassargues (2006) could not be verified with measured concentrations or fluxes, the present study allowed demonstrating the effect of the heterogeneity of diffusion parameters on mass transport in low-permeability media on a case study where measured chloride concentrations are available.

Acknowledgments The authors wish to acknowledge the Fund for Scientific Research—Flanders for providing a Postdoctoral Fellowship to the first author. The authors thank IRSN for providing the necessary data for this study.

References

Acero P, Auque LF, Gimeno MJ, Gomez JB (2010) Evaluation of mineral precipitation potential in a spent nuclear fuel repository. Environ Earth Sci 59(8):1613–1628

Ball WP, Liu C, Xia G, Young DF (1997) A diffusion-based interpretation of tetrachloroethene and trichloroethene concentration profiles in a groundwater aquitard. Water Resour Res 33:2741–2757

Barnwart S, Wikberg P, Olsson O (1997) A testbed for underground nuclear repository design. Environ Sci Technol 31:510–514

Barone FS, Rowe RK, Quigley RM (1992) A laboratory estimation of diffusion and adsorption coefficients for several volatile organics in a natural clayey soil. J Contam Hydrolol 10:225–250

Boisson J-Y, Cabrera J, De Windt L (1998) Fluid flow through faults and fractures in argillaceous formations. In: OECD proceedings. Joint NEA/EC workshop on fluid flow through faults and fractures in argillaceous formations, Bern, Switzerland, 10–12 June 1996, pp 207–222

Boisson J-Y, Bertrand L, Heitz J-F, Moureau-Le Golvan Y (2001) In situ and laboratory investigations of fluid flow through an argillaceous formation at different scales of space and time, Tournemire tunnel, southern France. Hydrogeol J 9:108–123

Bonin B (1998) Deep geological disposal in argillaceous formations: studies at the Tournemire test site. J Contam Hydrolol 35: 315–330

Bradbury KR, Eaton TT, Gotkowitz MB, Hart DJ, Cherry JA, Parker BL, Borchardt MA (2006) Contaminant transport through aquitards: technical guidance for aquitard assessment. AWWA Research Foundation, Denver

Bredehoeft JD, England AW, Stewart DV, Trask NJ, Winograd IJ (1978) Geologic disposal of high-level radioactive wastes - Earth science perspectives. US Geol Surv Circ 779:1–15

Bredehoeft JD, Neuzil CE, Milly PCD (1983) Regional flow in the Dakota Aquifer: a study of the role of confining layers. US Geol Surv Water Supply Pap 2237:1–45

Cherry JA, Parker BL, Bradbury KR, Eaton TT, Gotkowitz MB, Hart DJ, Borchardt MA (2006) Contaminant transport through aquitards: a state of the science review. AWWA Research Foundation, Denver

Crooks VE, Quigley RM (1984) Saline leachate migration through clay: a comparative laboratory and field investigation. Can Geotech J 21:349–362

Desaulniers DE, Cherry JA, Fritz P (1981) Origin, age and movement of pore water in argillaceous quaternary deposits at four sites in southwestern Ontario. J Hydrol 50:231–257

Desaulniers DE, Kaufman RS, Cherry JA, Bentley HW (1986) ^{37}Cl–^{35}Cl variations in a diffusion-controlled groundwater system. Geochimica Cosmochimica Acta 50:1757–1764

Deutsch CV, Journel AG (1998) GSLIB geostatistical software library and user's guide. Oxford University Press, New York

Goodall DC, Quigley RM (1977) Pollutant migration from two sanitary landfill sites near Sarnia, Ontario. Can Geotech J 14:223–236

Horseman ST, Higgo JJW, Alexander J, Harrington JF (1996) Water, gas and solute movement through argillaceous media. Nuclear Energy Agency, Organisation for Economic Co-operation and Development, Paris

Hummel W, Schneider JW (2005) Safety of nuclear waste repositories. Chimia 59(12):909–915

Huysmans M, Dassargues A (2005) Review of the use of Péclet numbers to determine the relative importance of advection and diffusion in low permeability environments. Hydrogeol J 13(5–6):895–904

Huysmans M, Dassargues A (2006) Stochastic analysis of the effect of spatial variability of diffusion parameters on radionuclide transport in a low permeability clay layer. Hydrogeol J 14(7):1094–1106

Huysmans M, Dassargues A (2007) Equivalent diffusion coefficient and equivalent diffusion accessible porosity of a stratified porous medium. Transp Porous Media 66(3):421–438

Isaaks EH, Srivastava RM (1989) An introduction to applied geostatistics. Oxford University Press, New York

Johnson RL, Cherry JA, Pankow JF (1989) Diffusive contaminant transport in natural clay: a field example and implications for clay-lined waste disposal sites. Environ Sci Technol 23:340–349

Larrondo P, Deutsch CV (2004) Accounting for geological boundary uncertainty for simulation of multiple rock types. In: Proceedings of Geostats2004, the seventh international geostatistics congress, September 26–October 1, 2004, Banff, Canada

Mallants D, Marivoet J, Sillen X (2001) Performance assessment of the disposal of vitrified high-level waste in a clay layer. J Nucl Mater 298(1–2):125–135

Mazurek M, Alt-Epping P, Bath A, Gimmi T, Waber HN, Buschaert S, De Cannière P, De Craen M, Gautschi A, Savoye S, Vinsot A, Wemaere I, Wouters L (2011) Natural tracer profiles across argillaceous formations. Appl Geochem 26:1035–1064

Neuman SP, Witherspoon PA (1972) Field determination of hydraulic properties of leaky multiple aquifer systems. Water Resour Res 8(5):1284–1298

Neuzil CE (1986) Groundwater flow in low-permeability environments. Water Resour Res 22:1163–1195

Oz B, Deutsch CV, Tran TT, Xie Y (2003) DSSIM-HR: a FORTRAN 90 program for direct sequential simulation with histogram reproduction. Comput Geosci 29(1):39–51

Patriarche D, Michelet J-L, Ledoux E, Savoye S (2004a) Diffusion as the main process for mass transport in very low water content argillites: 1. Chloride as a natural tracer for mass transport—diffusion coefficient and concentration measurements in interstitial water. Water Resour Res 40(1):W01517. doi:10.1029/2003WR002700

Patriarche D, Ledoux E, Michelet J-L, Simon-Coinçon R, Savoye S (2004b) Diffusion as the main process for mass transport in very low water content argillites: 2. Fluid flow and mass transport modelling. Water Resour Res 40(1):W01516. doi:10.1029/2003WR002600

Remenda VH, van der Kamp G, Cherry JA (1996) Use of vertical profiles of d18O to constrain estimates of hydraulic conductivity in a thick, unfractured aquitard. Water Resour Res 32:2979–2987

Ringwood AE (1985) Disposal of high-level nuclear wastes—a geological perspective. Miner Mag 49(351):159–176

Schwartz M (2009) Modelling groundwater contamination above the Asse 2 medium-level nuclear waste repository, Germany. Environ Earth Sci 59(2):277–286

Shackelford CD, Daniel DE (1991) Diffusion in saturated soil. I: background. J Geotech Eng 117:467–484

Therrien R, Sudicky EA (1996) Three-dimensional analysis of variably-saturated flow and solute transport in discretely-fractured porous media. J Contam Hydrol 23(1–2):1–44

Therrien R, Sudicky EA, McLaren RG (2003) FRAC3DVS: an efficient simulator for three-dimensional, saturated-unsaturated groundwater flow and density dependent, chain-decay solute transport in porous, discretely-fractured porous or dual-porosity formations. User's guide